applied sciences

MDPI

Article

Research on the Design Method of Cushioning Packaging for Products with Unbalanced Mass

Xiaojun Yang [1,2], Huoxing Li [1], Ying Sun [1], Yijie Cai [1,2,*], Hongdi Zhou [1,2] and Fei Zhong [1,2,*]

[1] School of Mechanical Engineering, Hubei University of Technology, Wuhan 430068, China; 19910055@hbut.edu.cn (X.Y.); 102110165@hbut.edu.cn (H.L.); woyingaini1314@163.com (Y.S.); zh_hongdi@163.com (H.Z.)

[2] Hubei Key Laboratory of Modern Manufacturing Quality Engineering, Hubei University of Technology, Wuhan 430068, China

* Correspondence: yijie.cai@hbut.edu.cn (Y.C.); zhong_fei_hbut@163.com (F.Z.); Tel.: +86-186-2705-8337 (Y.C.); +86-158-0716-3787 (F.Z.)

Abstract: The purpose of this work is to provide support for the design of cushioning packaging materials for products with unbalanced mass distributions. A mathematical model of the cushioning packaging system is established and the fourth-order Runge–Kutta method is used to compare the vibration response of products with balanced and unbalanced mass. Finite element simulations are conducted to demonstrate the feasibility of the proposed method of optimizing the design of cushioning packaging materials for products with unbalanced mass distributions using various damping materials. The simulation results are verified by experiments. The results show that the magnitude of the mass offset has a large effect on the acceleration of damped cushioning packaging systems for products with unbalanced mass. The vibration response can be corrected by appropriately increasing the damping coefficient at the mass offset end, thus providing an effective method of optimizing the design of cushioning packaging for products with unbalanced mass.

Keywords: unbalanced mass; damping materials; vibration response; cushioning packaging

check for updates

Citation: Yang, X.; Li, H.; Sun, Y.; Cai, Y.; Zhou, H.; Zhong, F. Research on the Design Method of Cushioning Packaging for Products with Unbalanced Mass. *Appl. Sci.* **2023**, *13*, 8632. https://doi.org/10.3390/app13158632

Academic Editor: Arkadiusz Gola

Received: 9 May 2023
Revised: 4 July 2023
Accepted: 24 July 2023
Published: 26 July 2023

Copyright: © 2023 by the authors. Licensee MDPI, Basel, Switzerland. This article is an open access article distributed under the terms and conditions of the Creative Commons Attribution (CC BY) license (https://creativecommons.org/licenses/by/4.0/).

1. Introduction

With the rapid development of the social economy, logistics transportation has become one of the important economic industries. Insufficient and excessive packaging may occur in the process of logistics transportation due to the various sizes [1], materials and categories of products [2], which may lead to product damage and cost increases, especially for some industrial precision instrument products. In order to ensure product transportation safe from impact and vibration [3,4], it is necessary to design and study the buffered packaging of products [5,6], especially for the precision optimization of products with centroid deviation (centroid and body centroid do not coincide). Continuously optimizing the design is important to reduce the damage of products and achieve packaging reduction [7].

Extensive research have been carried out into buffered packaging systems. Zhu et al. [8] focused on the cushion packaging system of products with a single degree of freedom as the research object and discussed the probability of the first incident of damage to the maximum displacement response, which provided theoretical support for the traversal damage probability of the maximum displacement of the product cushion-packaging system. As there are many types of cushioning structures in practical applications, and the application range of the single degree of freedom theory cannot cover all cushioning packaging systems, Li [9] studied two-degree-of-freedom dynamic models of suspension cushioning and packaging systems, explored the influence of buffered-packaging-system parameters on performance under falling conditions. Schell [10] analyzed the buffered packaging system with multiple degrees of freedom as the research object, established its response dynamic equation and measured the damaged boundary of buffered packaging

products with the back peak sawteeth acceleration pulse. Sun [11] developed a nonlinear differential equation of motion of the buffered packaging system based on the Lagrange general dynamics equation, and solved the nonlinear differential equation by means of equal method, Markov method, perturbation method and simulation method. Li et al. [12] evaluated the strong nonlinearity of the buffered packaging dynamics model using MMA and HAM algorithms and validated their accuracy through experiments. For the study of the vibration-response characteristics of buffered packaging, Hao [13] refined the vibration response characteristics of buffered packaging, focusing on the buffered packaging characteristics of vulnerable parts such as cantilever beams. Sakara [14] investigated a buffered package containing cantilever beams. He discussed the effects of axial force position and the number of spring-mass systems on the system's natural frequency under axial force. Yang et al. [15] established the dynamic equation of the system based on BP neural network and solved it using Runge–Kutta algorithm. A multi-objective optimization model for series buffering systems and an examination of factors impacting system performance was developed. Rong [16] takes a new type of buffered packaging material X-PLY corrugated cardboard as the research object; X-PLY corrugated cardboard is usually made into buffer pads (sheets), used in the field of logistics transportation packaging, to protect internal products from shock and vibration. In the actual logistics process, external vibration excitation often causes package resonance and leads finally to damage of the package. In order to understand its natural frequency and vibration mode, Lanczos modal analysis method was used in ANAYS simulation software to obtain the natural frequency and vibration mode of X-PLY corrugated cardboard cushion under three different static stresses. As for the study of objects with centroid migration, Gao [17] established the dynamic equation of a buffered packaging system under half sinusoidal acceleration pulses. They investigated rotation issues caused by product centroid migration and studied the coupling problem between rotation and translation, providing insights for buffered packaging system design and optimization. Yue [18] conducted a study on the eccentricity of driven piles in the construction industry. He analyzed cases where the piles deviated from their expected position and discussed the lateral movement caused by basement excavation. The study investigated the influence of lateral movement on pile foundation design and proposed appropriate allowable eccentric distances for driven piles in basement development. Ahmad et al. [19] studied the efficiency of torsional tuned mass dampers (T-TMDs) in asymmetric building response control under bidirectional seismic ground excitation. They evaluated damper efficiency by calculating rotation, displacement and acceleration, studying parameters of various configurations. Their findings confirmed that torsional tuned mass dampers are effective in reducing torsional responses in asymmetric buildings. Du [20] conducted a comparative analysis of commonly used buffering packaging materials. The study generated vibration-reduction curves for each material and provided references for buffered packaging system design and research. Experimental verification was performed to assess the influence of buffering packaging materials on structure design and vibration-reduction capabilities. Cho et al. [21] discovered that recycling waste tires can enhance the buffering effect of railway transportation packaging. They verified the relationship between tire thickness and vibration-reduction effects through relevant tests. Khalil et al. [22] focused on foam buffer materials. They developed a packaging selection diagram to quickly determine the optimal density of buffer materials based on the maximum stress the packaging system can bear. Zhang [23] designed a cushion packaging system for gas stove products using foam cushion gaskets. The impact and vibration-response results were analyzed, with a primary focus on studying the impact response of cushion gaskets. Li [24] conducted relevant research on the buffered packaging of range hoods. The packaging was redesigned using traditional EPS buffer materials to reduce weight while meeting product brittleness requirements, as rangehoods are prone to damage. Ge et al. [25], aiming at cost-effectiveness, relied on 3D printing to obtain relevant buffer structures, and studied material selection and the buffer performance of two structural models.

The above studies mainly focus on the vertical vibration shock, ignoring the lateral vibration shock caused by the change. Unbalanced products can lead to centroid shift in the horizontal direction, resulting in different vibration responses at different horizontal positions. Moreover, the eccentric distance of the product with unbalanced mass in the horizontal direction will affect the acceleration-response amplitude, and a larger eccentric distance will lead to a larger vibration-response acceleration. Therefore, it is necessary to optimize the vibration response of the system at different positions in the horizontal direction to reduce the acceleration-response amplitude. Unlike a mass-balanced product, which mainly has vertical vibration, a mass-unbalanced product will also rotate in the horizontal direction. This rotation can further increase the dynamic stress and strain caused by vibration, which in turn increases the risk of product breakage. At the same time, the theoretical or experimental modeling is often simplified by taking balanced quality products as the object. If the buffered packaging design intended for balanced products is directly applied to unbalanced products, it can lead to issues such as inadequate or excessive packaging. Some studies focus on the effect of centroid migration on the buffered characteristic response, but do not further optimize the difference of product response caused by centroid migration. For example, Cai [26] et al. focused on the cushioning characteristics of soft-landing airbags for UAVs. This study focused on analyzing the impact of centroid migration on the cushion characteristics of the air bag; for example, centroid migration may lead to changes in pressure distribution and deformation of the air bag. However, in this study, they did not delve into how to further optimize the differences in product response caused by centroid migration. Qi [27] et al. focused on developing experimental methods to evaluate the cushioning performance of the lander. In this case, the authors focus more on the impact of various factors on the buffer characteristics of the lander, rather than specifically on how to further optimize the differences in product response caused by centroid migration. Especially when the size and weight of the product is large, the centroid deviation will be more obvious, and because most buffered packaging uses the same symmetrical material structure, the buffer effect of unbalanced quality products is insufficient or excessive, and cannot really achieve packaging reduction.

A major challenge in this research is how to make full use of existing buffer materials and design methods in the actual production environment, and at the same time address the impact of centroid shift on vibration response. However, there are gaps in the current research in the following aspects:

1. There is a lack of in-depth research on the optimization method of buffered packaging design for unbalanced products. The existing research mainly focuses on the selection of buffer materials and the improvement of packaging structure, but there is no in-depth discussion on how to comprehensively consider various constraints and achieve the best design scheme in practice.
2. There is a lack of practical validation and case studies on the design of buffered packaging for unbalanced products. Most of the current studies rely on theoretical models and numerical simulations, and lack of verification of actual production scenarios. Therefore, it is important to obtain more data and cases from real environments to verify and evaluate the feasibility and validity of proposed design methods. This study aims to propose solutions for the design of cushioning packaging for unbalanced products.

In this paper, the cushioning and packaging system of unbalanced products is studied. We build a buffered packaging system model and analyze the effects of centroid migration on the acceleration amplitude and the problems related to the system response. The optimization of the installation method on the performance of buffering packaging system for unbalanced products is studied. We chose to use only expanded polyethylene (EPE) as the damping material for the experiment. Expanded polyethylene (EPE) is a commonly used material in buffered packaging systems because of its good damping properties and lightweight properties. Based on the good ability of expanded polyethylene to absorb energy and disperse vibration, we chose it as a damping material to optimize the system

effect and mitigate the impact on uneven products. Although only EPE is discussed in this study, other foams and asymmetric cushioned packaging structures may have an impact on system performance. However, due to time and resource constraints, we were unable to fully explore these factors in this study. We leave these exploratory studies for further investigation in the future.

2. Comparative Analysis of Vibration Response of Products with Balanced and Unbalanced Masses

The buffer material on the bottom of a product can provide support, fixation, and isolate vibrations. In practical engineering applications, the structure of the buffer material cannot be arbitrarily adjusted, and it is constrained by the shape and size of the bottom of the product. The same buffer material is often used to ensure the relative level of the bottom of the product. Therefore, the base of the buffered packaging system is often imbued with the same stiffness and the same vibration-damping materials to simplify the system.

First, a type of dimensional model of the cushioned packaging part is established as illustrated in Figure 1. G' represents the center of gravity of the product. The coordinate system is established with the center of gravity as the origin, and its direction is marked as the left direction. Symbols l_1, l_2, h_1, h_2, w_1 and w_2 represent the distance from center of mass G' to each side of the part. If $w_1 = w_2$ and $h_1 = h_2$, the center of mass and the body center are the same. Otherwise, the center of mass deviates from the body center and the product is in mass non-equilibrium, which produces a center-of-mass offset. Since the analysis is based on total energy, the displacement of the four support points in the direction of each coordinate axis must be calculated to obtain the forces of the spring-damper model. Taking center of mass G' as the origin to establish the coordinate axes, the length of each side is shown in Figure 1. The displacement of the center of mass along the coordinate axis directions are x, y, and z, respectively, and the angle of rotation around the coordinate axes are α, β, and γ, respectively. After analysis, the coordinates of the four-support points A, B, C, and D on the bottom surface are as follows.

$$\begin{aligned} x_a &= x + l_2\beta + h_2\gamma,\ y_a = y - l_2\alpha - w_1\gamma, z_a = z + w_1\beta - h_2\alpha \\ x_b &= x + l_2\beta + h_2\gamma,\ y_b = y - l_2\alpha + w_2\gamma, z_b = z - w_2\beta - h_2\alpha \\ x_c &= x - l_1\beta + h_2\gamma,\ y_c = y + l_1\alpha + w_2\gamma, z_c = z - w_2\beta - h_2\alpha \\ x_d &= x - l_1\beta + h_2\gamma,\ y_d = y + l_1\alpha - w_1\gamma, z_d = z + w_1\beta - h_2\alpha \end{aligned} \tag{1}$$

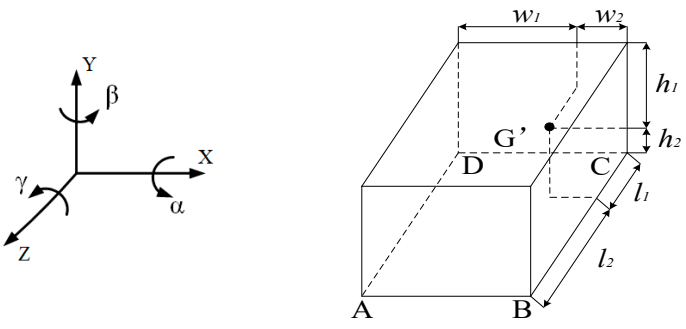

Figure 1. Size model.

The modeling process is performed by attaching counterweight blocks on both sides of the product, which causes the center of mass to deviate from the geometrical center. The simplified model is shown in Figure 2. The parameters k_i (i = 1, 2, 3, 4) and c_j (j = 1, 2, 3, 4) indicate spring stiffness and damping coefficient, respectively.

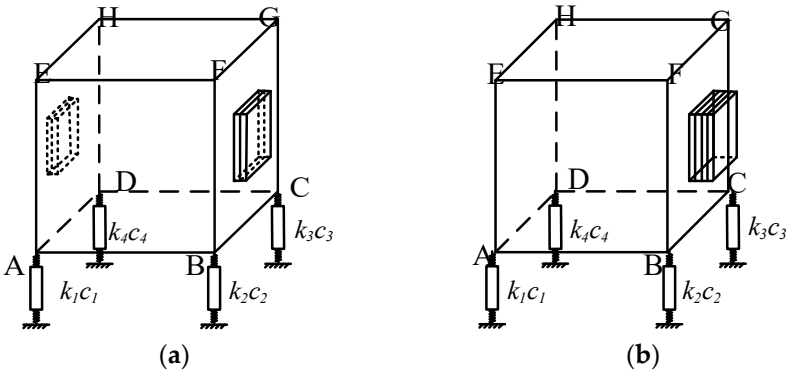

Figure 2. Simplified model. (**a**) Mass-balanced product model. (**b**) Mass-unbalanced product model.

Simplified models of products with balanced mass and unbalanced mass are all shown in Figure 2. An energy analysis is performed using the same initial conditions. In the case of the mass-balanced product, only translational motion in the y-direction occurs in the cushioning packaging system. In the case of mass non-equilibrium product, translational motion occurs in the y-direction as well as rotation in the z-direction. The kinetic energy, elastic potential energy, dissipative energy and total energy of packing system with balanced mass are set as T_1, V_1, U_1, and E_1, respectively, and those of packing system with unbalanced mass are set as T_2, V_2, U_2 and E_2, respectively.

The related parameters above are calculated as follows:

$$T_1 = \frac{1}{2}(M+m)\dot{y}^2 \tag{2}$$

$$T_2 = \frac{1}{2}(M+m)\dot{y}^2 + \frac{1}{2}J_z\dot{\gamma}^2 \tag{3}$$

$$v_1 = \frac{1}{2}k_1y^2 + \frac{1}{2}k_2y^2 + \frac{1}{2}k_3y^2 + \frac{1}{2}k_4y^2 \tag{4}$$

$$v_2 = \frac{1}{2}k_1(y-w_1\gamma)^2 + \frac{1}{2}k_2(y+w_2\gamma)^2 + \frac{1}{2}k_3(y+w_2\gamma)^2 + \frac{1}{2}k_4(y-w_1\gamma)^2 \tag{5}$$

$$U_1 = \frac{1}{2}c_1y^2 + \frac{1}{2}c_2y^2 + \frac{1}{2}c_3y^2 + \frac{1}{2}c_4y^2 \tag{6}$$

$$U_2 = \frac{1}{2}c_1(y-w_1\gamma)^2 + \frac{1}{2}c_2(y+w_2\gamma)^2 + \frac{1}{2}c_3(y+w_2\gamma)^2 + \frac{1}{2}c_4(y-w_1\gamma)^2 \tag{7}$$

$$E_1 = \frac{1}{2}(M+m)\dot{y}^2 + \frac{1}{2}k_1y^2 + \frac{1}{2}k_2y^2 + \frac{1}{2}k_3y^2 + \frac{1}{2}k_4y^2 + \frac{1}{2}c_1y^2 + \frac{1}{2}c_2y^2 + \frac{1}{2}c_3y^2 + \frac{1}{2}c_4y^2 \tag{8}$$

$$E_2 = \frac{1}{2}(M+m)\dot{y}^2 + \frac{1}{2}J_z\dot{\gamma}^2 + \frac{1}{2}k_1(y-w_1\gamma)^2 + \frac{1}{2}k_2(y+w_2\gamma)^2 + \frac{1}{2}k_3(y+w_2\gamma)^2 \tag{9}$$

Based on the forced dynamics and impact dynamics equations, the vibration mechanics differential equation of the products with unbalanced mass can be obtained:

$$m\ddot{y} + 4c_y \times \dot{y} + 2c_y(w_2-w_1)\dot{\gamma} + 4k_y \times y + 2k_y(w_2-w_1)\gamma = 0 \tag{10}$$

where $\dot{y}$ and $\dot{\gamma}$ denote the velocity along the y-axis and the angular velocity of z-axis, respectively. Thus, the systematic vibration response of a product with balanced mass and unbalanced mass distribution can be compared under the same vibration-isolation conditions. Before solving Equation (10) using fourth-order Runge–Kutta methods [28], the differential equations with various degrees should be processed for reducing orders to

obtain four first-order differential equations when the bottom surface of the product of the system is isolated. y_1, y_2, y_3, and y_4 in Equations (11)–(14) represent the y-axis displacement, y-axis velocity, z-axis rotation angle, and z-axis angular velocity of the motion parameters, respectively. The mass-balanced and vibration response of the mass-unbalanced product are solved using Equation (15). The vibration response diagrams are shown in Figure 2a,b. The derivatives of y_1, y_2, y_3, and y_4 are:

$$\dot{y}_1 = y_2 \tag{11}$$

$$\dot{y}_2 = \frac{1}{m}\left(-2c_y(w_2 - w_1)y_4 - 4k_y y_3 - 2k_y(w_2 - w_1)y_3\right) \tag{12}$$

$$\dot{y}_3 = y_4 \tag{13}$$

$$\dot{y}_4 = \frac{1}{J_z}\left(-2c_y\left({w_1}^2 + {w_2}^2\right)y_4 - 2k_y(w_2 - w_1)y_1 - k_y\left({w_1}^2 + {w_2}^2\right)y_3\right) \tag{14}$$

The solutions of the vibration differential equations of mass-balanced and mass-unbalanced products are:

$$\begin{aligned} y_{unbalanced} = {} & C_1 e^{x\times(\mu+\sqrt{\eta-\zeta})/\phi} + C_2 e^{x\times(\mu-\sqrt{\eta-\zeta})/\phi} + [e^{x\times(\mu+\sqrt{\eta-\zeta})/\phi} \times \int e^{-x\times(\mu+\sqrt{\eta-\zeta})/\phi} f(x)dx \\ & - e^{x\times(\mu-\sqrt{\eta-\zeta})/\phi} \times \int e^{-x\times(\mu-\sqrt{\eta-\zeta})/\phi} f(x)dx]/4\sqrt{\eta-\zeta} \end{aligned} \tag{15}$$

$$\begin{aligned} y_{balanced} = {} & C_1 e^{x\times\frac{\mu+\sqrt{-\zeta}}{\phi}} + C_2 e^{x\times\frac{\mu-\sqrt{-\zeta}}{\phi}} + [e^{x\times\frac{\mu+\sqrt{-\zeta}}{\phi}} \times \int e^{-x\times\frac{\mu+\sqrt{-\zeta}}{\phi}} f(x)dx \\ & - e^{x\times(\mu-\sqrt{-\zeta})/\phi} \times \int e^{-x\times(\mu-\sqrt{-\zeta})/\phi} f(x)dx]/4\sqrt{-\zeta} \end{aligned} \tag{16}$$

where

$\mu = 2c_y\left[c_y w_1 w_2 - J_z - 2c_y\left({w_1}^2 + {w_2}^2\right)\right]$

$\eta = c_y(w_1 - w_2)^2[J_z\left(k_y(m+M) - 2{c_y}^2\right) - c_y \times \left({w_1}^2 + {w_2}^2\right) \times (2w_1 w_2 {c_y}^3 + 4{c_y}^2 - c_y + 2(m+M)k_y)]$

$\zeta = \left[(m+M)k_y - {c_y}^2\right](2c_y \times {w_1}^2 + {w_2}^2 + J_z)^2$

$\phi = \left[J_z + 2c_y\left({w_1}^2 + {w_2}^2\right)\right] \times (m+M)$

Analytical comparison of the solutions of the vibration differential equation for the mass-unbalanced product and mass-balanced product shows that the differences of the solutions between Equations (15) and (16) depend on the magnitude of the eccentric distance. When $w_1 - w_2 = 0$, the mass of the product distributes uniformly in its space and the mass center of the system is not offset. However, the mass of the product is not distributed uniformly in its own space and the mass center of the system is derived from its geometrical center when $w_1 - w_2$ is not equal to 0. The exponential part of the theoretical solution of the differential equation for solving the vibration response changes obviously and the vibration responses of the mass non-equilibrium product and mass-balanced product are different. The larger the eccentricity, the larger the difference in the vibration response.

Next, fourth-order Runge–Kutta methods are used to numerically solve the vibration response. In this study, the total mass ($M + m$) of the package is set to 10 kg, the spring stiffness coefficients k_1, k_2, k_3 and k_4 are all set to 1.5 N/m, and the damping coefficients c_1, c_2, c_3 and c_4 are all set to 1.5 N·s/m.

As seen in Figure 3, when balanced and unbalanced products with the same mass and size vibrate under the same conditions, the vibration characteristics of the mass-balanced product are more stable, and the positive and negative response amplitudes are symmetrical and gradually decrease. The overall trend in the vibration response of the non-equilibrium product is also gradually decaying, and the positive and negative response amplitudes are symmetrical. However, the response amplitudes fluctuate periodically in local area. The

difference between the response amplitude of the mass-unbalanced product and the mass-balanced product is about 45.5% at 0.15 s. The difference is caused by the shift in center-of-mass of the mass-unbalanced product, which produces rotational energy in the z-direction, thereby increasing the total energy compared with the mass-balanced product. The positive and negative magnitudes of the unbalanced product are much larger than those of the mass-balanced product, which is consistent with the theoretical solution. It can be derived that there is a large difference between the mass-balanced and mass-unbalanced products in terms of the vibration response results and trends according to Equations (15) and (16) and Figure 3. Moreover, when the same vibration-isolation and cushioning design are applied to the mass-balanced and mass-unbalanced products, such as our experimental design using the same damping material thickness, density and product system, the packaging system does not meet the vibration isolation and cushioning requirements of the unbalanced product, which may lead to breakage during the transportation process. Therefore, we can consider choosing a buffer material with better damping characteristics to optimize the buffered packaging design, and can study the performance differences of the buffered packaging system under different thickness, density and other parameters by experiment. According to the periodic fluctuation of non-equilibrium-product vibration response, the layout of buffer material can be adjusted to reduce the fluctuation of response amplitude. According to the difference of response amplitudes between unbalanced and balanced products in Figure 3, a buffer-structure stiffness more suitable for unbalanced products can be designed to achieve the purpose of optimizing the buffered packaging design of unbalanced products.

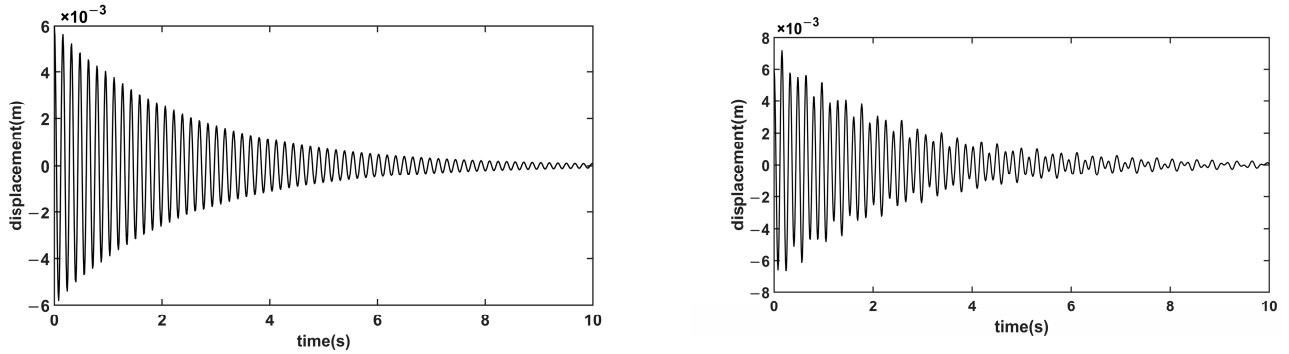

Figure 3. Comparison of vibration response of product with balanced and unbalanced mass. (**a**) Mass-balanced. (**b**) Mass-unbalanced.

3. Analysis of Response for Damping Material to Center-of-Mass Offset System

Since damping materials have good corrosion-resistance, vibration-damping, and anti-buffering properties, damping vibration-isolation materials are used to correct the vibration response of a mass-unbalanced product in this paper. When four counterweight blocks are adopted and the center of the left sides or right sides are symmetrically installed, then the center of mass can be derived from its geometrical center, λ_x = 19.79 mm. Similarly, when eight counterweight blocks are asymmetrically installed, the center of mass is offset by λ_x = 35.88 mm. When 16 blocks are installed, the eccentric distance is λ_x = 83.69 mm.

First, the different theoretical models corresponding to different offset distances of the center of mass are simulated and analyzed by applying workbench [29,30]. Following this, a harmonic response analysis is carried out [31,32]. In addition, the peak acceleration response is discussed according to the frequency acceleration curves. In this paper, the frequency is set to be from 3 to 21 Hz and the acceleration is set to 1 m/s^2 in y direction. The theoretical model is shown in Figure 4, and the material parameters are listed in Table 1.

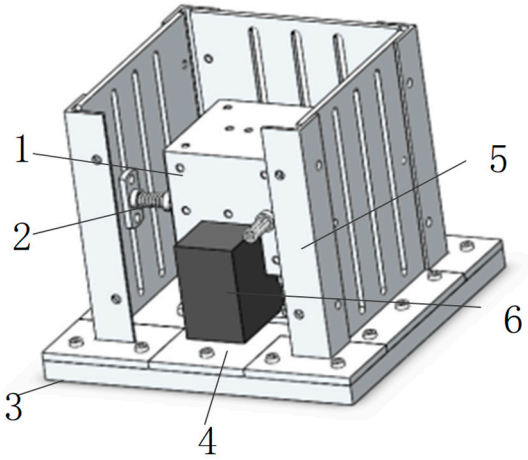

Figure 4. Theoretical model. 1—object block. 2—spring vibration isolator. 3—shaker tabletop. 4—clamp plate. 5—angular aluminum fixings. 6—damping blocks.

Table 1. Properties of material.

Name	Materials	Density (kg/m^3)	Young's Modulus (MPa)	Poisson's Ratio
Object	Aluminum alloy	2770	7.1×10^4	0.33
Counterweight block	Structural steel	7850	2.0×10^5	0.30
Vibration Isolators	AISI304	8000	1.9×10^{11}	0.29
Damping material	EPE	16	5.5×10^5	0.10

A harmonic response is added to simulate the effect of a cushioning material on the cushioning characteristics of a mass-eccentric system. The effect of changing relevant parameters of the same cushioning packaging material, i.e., the area, thickness and density of the damping material, on the cushioning characteristics of the mass-eccentric system is analyzed when the quality of product packaging is maintained at a certain level. The results of the dynamic response of the mass-eccentric system, with different parameters that have the same cushioning-damping packaging material, are shown in Table 2.

Table 2. Response results of packaging systems for unbalanced -mass products with different structural parameters of the same damping packaging material.

Density (kg/m^3)	Length/Width (mm)	Area (mm^2)	Thickness (mm)	Damping Factor (N·s/m)	Maximum Acceleration (m/s^2)	Difference Ratio (%)
16	75/80	6000	50	2.59	6.75	+14.2%
	50/80	4000	50	2.67	5.33	−9.8%
	25/80	2000	50	2.89	5.82	−1.5%
	60/80	4800	50	2.54	7.12	+20.4%
	50/80	4000	40	2.73	2.78	−52.9%
	50/80	4000	30	3.14	5.28	−10.6%
18	75/80	6000	50	2.69	6.28	+6.3%
	50/80	4000	50	2.61	6.57	+11.2%
	25/80	2000	50	2.85	6.05	+2.4%
	60/80	4800	50	2.74	6.18	+4.5%
	25/80	2000	40	2.93	2.61	−55.8%
	25/80	2000	30	3.24	5.04	−14.7%

Here, the ratio in Table 2 is the ratio between the acceleration amplitude of the mass-unbalanced product with different damping-installation methods to the maximum acceleration with the same balanced mass without damping-optimized installation.

The parameters in Table 2 are based on commonly used buffered-packaging design parameters for experimental design. In this study, we studied the vibration response of products with unbalanced mass by changing the thickness, width, height and density of damping materials. The data in Table 2 show the vibration response of the mass unbalanced product with the same damping-material characteristics. It can be observed from the data in Table 2 that there are differences in the maximum acceleration under different thickness conditions. Comparing the data at larger thicknesses (50 mm) and smaller thicknesses (40 mm and 30 mm), it can be find that the maximum acceleration at larger thicknesses is relatively small. This may be due to the fact that the larger thickness provides greater structural stability and reduces the energy loss from vibration conduction. Therefore, in the case of a need to improve the stability of the system, it may be more appropriate to choose a larger thickness. The maximum acceleration under high-density conditions is relatively large. Comparing the data under different density conditions, it can be seen that a density of 16 kg/m^3 can achieve a higher maximum acceleration than a density of 18 kg/m^3. The higher density may provide better energy-absorption and transfer characteristics, thereby reducing the effects of vibration. However, the choice of thickness and density is limited by the cost and feasibility of the material, so it needs to be considered comprehensively, and it can be observed from the data that the impact of changes in width and height on the performance of the system is not obvious. There is no clear trend or pattern in the data in Table 2. This means that in this experiment, changes in width and height have a small effect on system performance, and further research is needed to explore the mechanism of their influence.

The vibration responses of mass-unbalanced products with the same damping-material properties are presented in Table 2. Keeping the density and thickness of the damping material at 16 kg/m^3 and 50 mm, respectively, the contact areas of the structure of the damping material are respectively set as the corresponding magnitude. On one hand, the response amplitude of acceleration of the mass-unbalanced system with area of 4000 mm^2 is obviously decreased compared to that of one of 6000 mm^2 and 2000 mm^2. Moreover, the response amplitude of acceleration of the mass-unbalanced system with area of 4000 mm^2 is decreased by 9.8% compared to that of the mass-unbalanced system without damping material. On the other hand, when keeping the area of the damping material to be 4000 mm^2 and changing the thickness of the damping material, the amplitude of the acceleration of the vibration response is decreased by 52.9% when the thickness is 40 mm. Similarly, when the density, thickness and area of the damping material is 18 kg/m^3, 50 mm and 2000 mm^2, respectively, the response amplitude of the acceleration is 6.05 m/s^2. However, when the thickness of damping buffer material is changed and set to be 40 mm, the corresponding response amplitude of the acceleration is 2.61 m/s^2, which is decreased by 55.8% compared with that of the mass-unbalanced system without damping material.

Until now, a theoretical model based on different parameters of material above has been formulated. However, different damping materials with different damping coefficients have different effects on the cushioning characteristics of the mass-unbalanced system. In detail, the effects of the changing coefficients of the damping materials near to and away from the center of mass on the vibration-response results are listed in Table 3.

Here, the ratio presented in Table 3 is the ratio between the acceleration amplitude of the mass-unbalanced product with the damping material and the maximum acceleration under the same conditions without the damping material.

As shown in Table 3, the eccentric distance is 19.79 mm, and the acceleration-response amplitude of the mass-unbalanced product is 5.91 m/s^2 under the optimized condition with no damping vibration-isolation material. The amplitude of acceleration response of the mass-unbalanced product with no damping vibration-isolation material is 5.91 m/s^2 when the eccentric distance is 19.79 mm.

Table 3. Response results of packaging systems for mass-unbalanced products with different damping packaging materials.

Product Mass (kg)	Eccentric Distance (mm)	Damping Factor at the Distal Center of Mass (N·s/m)	Damping Factor Near the Center of Mass End (N·s/m)	Maximum Acceleration (m/s^2)	Difference Ratio (%)
9	19.79	0	0	5.91	-
	19.79	2.5	2.5	5.73	−3.0%
	19.79	2.5	2.6	5.51	−6.7%
	19.79	2.4	2.5	5.68	−3.9%
	19.79	2.5	2.4	5.88	−0.5%
11	35.88	2.7	2.7	9.98	−17.2%
	35.88	2.7	2.8	9.05	−24.9%
	35.88	2.6	2.7	10.59	−12.1%
	35.88	2.8	2.7	11.33	−6.0%
	35.88	0	0	12.05	-
15	83.69	0	0	20.68	-
	83.69	3.1	3.1	15.79	−23.6%
	83.69	3.1	3.2	11.26	−45.6%
	83.69	3.0	3.1	14.32	−30.7%
	83.69	3.2	3.1	17.65	−14.6%

When the eccentric distance remains unchanged and the damping material is added to the mass-unbalanced product, the acceleration-response amplitude is significantly reduced. The acceleration-response amplitude is 5.73 m/s^2 when the damping coefficient of material is 2.5 N·s/m near to and far from the center-of-mass, respectively, resulting in a decrease of 3.0% compared with that of the material with undamped vibration isolation. Hence, the stresses near to and far away from the center of mass of the mass-unbalanced system are different.

The damping coefficients of the material near to and far away from the center of mass can be adjusted appropriately to correct the response. After the damping coefficient of the material near the center of mass is increased, the amplitude of acceleration of the vibration response is decreased by 6.7%.

The amplitude of the acceleration response is decreased by 0.5% when the damping coefficient near the center of mass is decreased. When the eccentric distance λ_x and the damping coefficient of the material near to and far away from the center of mass are 35.88 mm and 2.5 N·s/m respectively, the amplitude of the acceleration response is 9.98 m/s^2. Thus, the amplitude of the vibration response significantly decreases when the damping coefficient of the material near the center-of-mass is increased. The scaled-up and scaled-down model data show that the use of vibration-isolation materials with larger damping coefficients near the center of mass end is feasible to correct the vibration response.

The above results show that the mass deflection has a large impact on the acceleration-response amplitude, and the cushioning-damping packaging material has a certain positive effect on its cushioning characteristics. The damping coefficient decreases with the increase in thickness within a certain range, and the thicker the thickness, the better the vibration-isolation effect. Changing the packing material and the damping coefficient also has a certain effect on the dynamic characteristics of the mass-unbalanced system; especially when a larger damping coefficient material is used near the eccentric end, the acceleration response tends to decrease more significantly.

4. Experimental Design and Analysis

Static compression tests were conducted on EPE with different densities according to Chinese National Standard GB/T 8168-2008 [33], which is a static compression test method for packaging cushioning materials, as shown in Figure 5. The size and number of test samples are taken as a regular 100 mm × 100 mm histograms.



Figure 5. Static compression test.

Figure 6 shows that below a certain strain value, the stress–strain relationship is linear, and the stress is less than the yield limit, i.e., the material is in the elastic deformation stage. For the same strain value, the stress corresponding to the EPE of higher density is higher, the energy absorbed by the material is also higher. The effect of different densities on the vibration response of the cushioning packaging system for mass non-equilibrium products is experimentally studied.

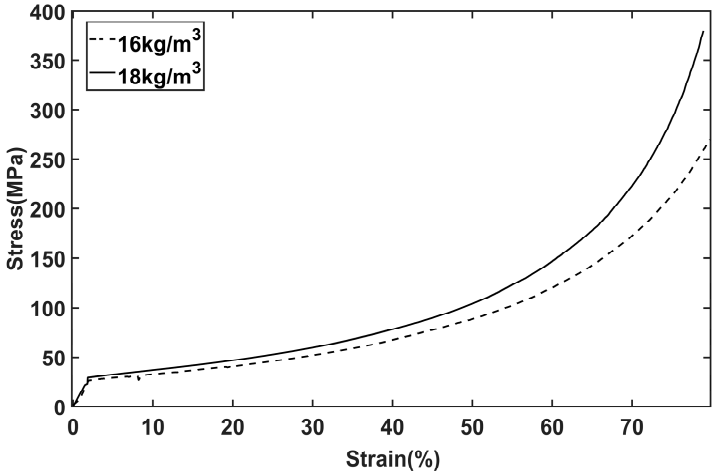

Figure 6. Stress–strain curves.

The damping material was cut with a hand knife and standard ruler into different areas and different thicknesses as shown in Figure 7 for a sine sweep experiment. The experimental apparatus shown in Figure 8 consisted of an aluminum alloy block (20 cm × 20 cm × 20 cm) with a mass of 9 kg, a cushioning vibration-isolation material, a counterweight block, and a sensor. The block was smoothly connected to a Suzhou DY300-3 vibration test rig [34] via the vibration-isolation material and a transducer was attached to the block using an instantaneous dry glue. To ensure the reliability of the experimental results, the experiment was repeated three times, and the average values were calculated. This approach helps to reduce the influence of random factors and increases the statistical significance of the obtained data. A sinusoidal sweeping experiment [35] is conducted by applying an excitation of 1 m/s^2 to the block along the y-direction and longitudinal acceleration curves of the buffered packaging system are obtained for mass-balanced and mass-unbalanced products with different vibration-isolation material installation methods.



Figure 7. Different sizes of EPE material.

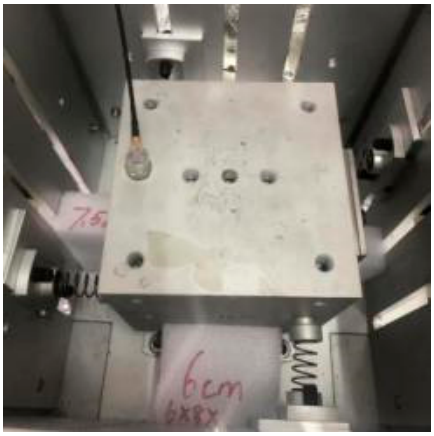

Figure 8. Physical model.

Figure 9 shows the vibration-response results of a mass-unbalanced-product packaging system under different buffered-packaging-material densities. The thickness of the damping material is set to a constant 50 cm, and the length x width, i.e., contact area, is varied. To maintain a minimum thickness of the damping material, dimensions of 75 cm × 80 cm, 50 cm × 80 cm, 25 cm × 80 cm, and 60 cm × 80 cm are tested, resulting in cushioning-packaging-system acceleration-response amplitudes of 5.92 m/s^2, 6.18 m/s^2, 5.69 m/s^2, 5.81 m/s^2, and 6.25 m/s^2, 4.94 m/s^2, 5.48 m/s^2, and 6.72 m/s^2, respectively, comparing the acceleration-response amplitudes for different areas of damping materials. Among them, the cushioning-packaging vibration-response effects of the larger density area, 25 cm × 80 cm, and the smaller density area, 50 cm × 80 cm, are better than for other areas, so the actual production life can be changed by the same kind of packaging damping material area to reduce the mass-unbalanced-product packaging-system acceleration-response amplitude.

To further explore the influence of packaging damping materials on the cushioning characteristics of mass-unbalanced systems, in Figure 10, the thickness of the damping material will be changed on the premise that the area of the damping material is certain.

The damped buffer material length and width are kept constant and the vibration response is modified by changing the thickness. According to the experimental results in Figure 10, it can be seen that when the thickness of the damping buffer material decreases, the acceleration-response amplitude of the packaging system of the unbalanced product will also decrease, and the corresponding frequency level of the acceleration amplitude will decrease accordingly. The acceleration-response amplitude is 5.69 m/s^2 for a 25 cm × 80 cm with dense damping materials, and the area remains the same. When the thickness of EPE material is changed from 40 mm to 30 mm, the corresponding acceleration-

response amplitudes of product packaging system with unbalanced mass are 2.47 m/s^2 and 4.73 m/s^2, respectively. Similarly, the acceleration-response amplitude is 4.94 m/s^2 for a 50 cm × 80 cm with less dense damping materials, and the area remains the same. When the thickness of EPE material is changed from 40 mm to 30 mm, the corresponding acceleration-response amplitudes of product packaging system with unbalanced mass are 2.62 m/s^2 and 5.03 m/s^2, respectively. Therefore, an appropriate increase in the thickness of the buffer material will reduce the amplitude of the acceleration response.

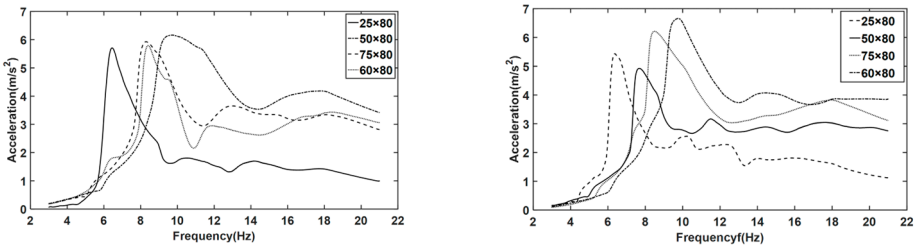

(**a**) (**b**)

Figure 9. Vibration-response curves for different areas of damping material. (**a**) Denser damping materials. (**b**) Less dense damping materials.

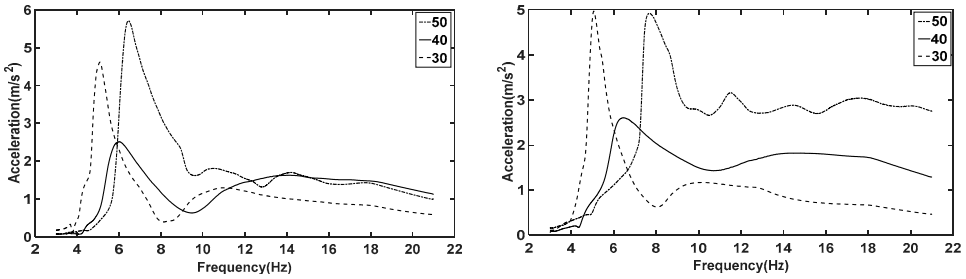

(**a**) (**b**)

Figure 10. Vibration-response curves for different thicknesses of packaging damping materials. (**a**) Denser damping materials. (**b**) Less dense damping materials.

In addition, the experiment also found that under the same thickness (40 mm), when the density of the damping material is large, the vibration-response amplitude of the mass unbalance system is the smallest, and the frequency level corresponding to the acceleration amplitude decreases. Specifically, when the area of the damping material is 2000 mm^2, the vibration-response amplitude is the smallest; when the area of damping material is 4000 mm^2, the amplitude of vibration response is relatively large. Therefore, it can be concluded that increasing the density of the buffer material will reduce the amplitude of the vibration response.

The results prove that the same packaging damping material can effectively reduce the acceleration-response amplitude of the packaging system and improve the buffering performance by only adjusting the geometric parameters, such as thickness and area, or increasing the density of the same material.

In addition, the vibration response of the near-center-of-mass and far-center-of-mass points of the mass-unbalanced-product packaging system also differed significantly. In order to discuss the location of the special parts of the product, this section will compare the vibration response of the near-, middle- and far-center-of-mass points of the mass-eccentric system with the above cushion packaging design method for a larger density of damping material, an area of 2000 mm^2 and a thickness of 40 mm. Compared with the vibration responses of the unbalanced-mass product at different positions, the vibration responses at the far center of mass, near center of mass, and surface midpoint of the unbalanced-mass product are analyzed by positioning sensors at points a, b and c, respectively, as shown in Figure 11; the placement of special parts can be subsequently determined.

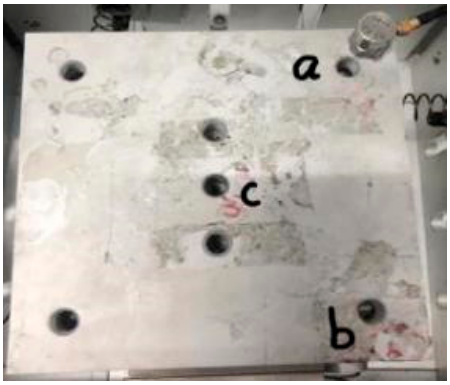

Figure 11. Positions of sensors.

Figure 12a,b show the vibration responses of the homogeneous product sensor without the EPE, and the endpoint and midpoint are not very different with a resonance frequency of 4.67 Hz and 4.86 Hz, respectively. The corresponding resonance-response amplitudes are 6.35 m/s^2 and 6.52 m/s^2. With EPE, the acceleration-response amplitudes corresponding to the resonance frequencies of 5.94 Hz and 5.89 Hz at the endpoint and midpoint of the homogeneous product position are 2.95 m/s^2 and 3.98 m/s^2, respectively. Figure 12c,d show the resonant frequencies of the acceleration sensor without the EPE at the near, middle and far center of mass of the non-homogeneous product are 5.1 Hz, 4.92 Hz and 5.19 Hz, respectively, corresponding to acceleration-response amplitudes of 6.9 m/s^2, 6.08 m/s^2 and 6.1 m/s^2. With EPE, the resonant frequencies at the near, middle and far center of mass of the non-equilibrium product are 5.59 Hz, 5.52 Hz and 5.36 Hz, respectively, corresponding to acceleration-response amplitudes of 2.91 m/s^2, 2.97 m/s^2 and 2.74 m/s^2.

The experimental results show the acceleration-response amplitudes do not change significantly among different locations on the mass-balanced product without damping. With the addition of the vibration isolation damping material, the acceleration-response amplitude significantly decreases and the resonance frequency changes. Therefore, the acceleration-response amplitude can be modified, and a resonance frequency region can be avoided in the design process of cushioning packaging systems by selecting certain damping conditions. Without the vibration-isolation damping material, the response amplitude at the near center of mass of non-homogeneous products increases by 13.5% compared with the far center of mass. Therefore, the distal center of mass is suitable for placing special parts compared with other locations for non-homogeneous products.

The vibration-response curves of the simulation and the experiment are consistent under the same damping material parameters. When the eccentric distance is 19.79 mm, the damping material density is 18 kg/m^3, the area is 2000 mm^2 and the thickness is 40 mm, the comparison of the simulation and experiment response curves can be seen in Figure 13. The fluctuation and acceleration amplitude of the simulation acceleration curve are consistent with the experimental results. Since the vibration performance of the vibration test bench has not reached the optimal stable state, there is a slightly larger error between the experiment results and the simulation results. As the vibration test bench equipment gradually enters the stable state, the peak value of the vibration-response curve is locally enlarged as shown in Figure 13. The vibration-response curve of the maximum acceleration amplitude of the simulation and the experiment results basically fit.

Observing the acceleration-response amplitude of simulation and experiment in Figure 14, where the eccentricity distance is (19.79 mm), and the structural parameters of damping materials are different, the experimental and simulated peak acceleration results under different structural parameters of damping materials are shown in Table 4.

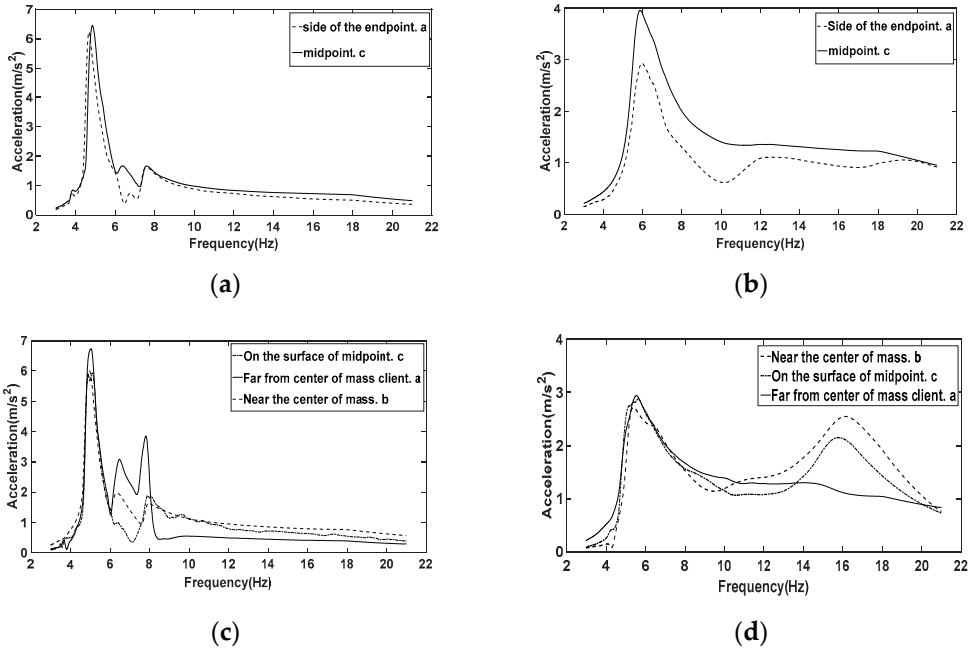

Figure 12. Curves for vibration response at different positions of sensors. (**a**) System for products with balanced mass before optimization. (**b**) System for products with balanced mass after being optimized by damping materials. (**c**) System for products with unbalanced mass before optimization. (**d**) System for products with unbalanced mass after optimized by damping materials.

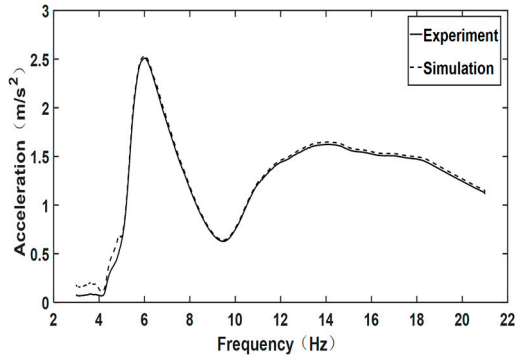

Figure 13. Comparison of simulation and experimental vibration curves.

a, b, c and d are density 16 kg/m^3, thickness 50 mm, area 6000 mm^2, 4000 mm^2, 2000 mm^2 and 4800 mm^2, respectively. e and f are density 16 kg/m^3, area 4000 mm^2, thickness 40 mm and 30 mm, respectively. A, B, C and D are density 18 kg/m^3, thickness 50 mm, area 6000 mm^2, 4000 mm^2, 2000 mm^2 and 4800 mm^2, respectively; E and F are density 18 kg/m^3, area 2000 mm^2 and thickness 40 mm and 30 mm, respectively. According to the amplitude curve of experiment and simulation acceleration response in Figure 14, a, b, c and d change the area of damping material when the density and thickness of damping material are constant. When the area is 4000 mm^2, the amplitude of the acceleration vibration response is the minimum 4.94 m/s^2. When the area of group A, B, C and D is 2000 mm^2, the amplitude of the minimum acceleration vibration response is 5.69 m/s^2. It can be seen that the damping material with larger density parameters has a smaller amplitude of vibration-acceleration response under the same damping factor. By comparing the simulation and experiment results of e and f and E and F, it can be seen that the thickness of the damping material is changed when the density and area of the damping material are constant. When the thickness parameter is 40 mm, the minimum vibration-acceleration-response amplitude is 2.62 m/s^2 and 2.47 m/s^2 respectively. It can be seen that the damping material with smaller thickness parameters has a smaller amplitude of

vibration-acceleration response under the same parameters. Based on the above analysis, the acceleration-response amplitude of the mass-unbalanced buffered packaging system can be effectively reduced by adjusting the geometric parameters, such as the area and thickness of the same packaging damping material, or using the same material to increase its density. According to the curve of the amplitude of vibration-acceleration response shown in Figure 14, there is about 10% difference between the simulated acceleration amplitude and the experimental result, which is caused by the performance of the vibration test bench itself and the interference of noise and vibration on the signal.

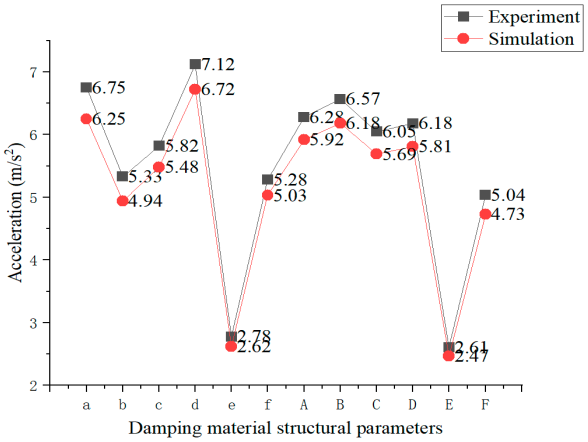

Figure 14. Comparison of simulation and experimental acceleration peaks using damping materials with different structural parameters.

Table 4. Damping materials with different structural parameters.

Difference Parameter	Density (kg/m^3)	Area (mm^2)	Thickness (mm)	Maximum Acceleration (Experiment) (m/s^2)	Maximum Acceleration (Simulation) (m/s^2)
a	16	6000	50	6.75	6.25
b	16	4000	50	5.33	4.94
c	16	2000	50	5.82	5.48
d	16	4800	50	7.12	6.72
e	16	4000	40	2.78	2.62
f	16	4000	30	5.28	5.03
A	18	6000	50	6.28	5.92
B	18	4000	50	6.57	6.18
C	18	2000	50	6.05	5.69
D	18	4800	50	6.18	5.81
E	18	2000	40	2.61	2.47
F	18	2000	30	5.04	4.73

By comprehensive comparison, it can be seen that the experimental simulation trend of the vibration response of the unbalanced buffered packaging system is similar under the same conditions, such as the eccentricity distance of the unbalanced product's mass, which further verifies the rationality of the simulation results.

5. Results and Discussion

We investigate and optimize the use of damping materials through experimental methods to correct the vibration response of unbalanced products. The results show that the acceleration response of buffered packaging systems is affected by centroid deviation. In addition, damping materials have a certain effect and can be used to correct the response. Fan [2] discusses the current situation and application of plastic buffered packaging materials. Although it does not specifically study the use of shock-absorbing materials, it

is consistent with our findings that the vibration response of packaging systems can be effectively reduced by changing the contact area and thickness of packaging materials. Both Lu [3] and Lu et al. [4] study the impact resistance of buffered packaging materials through finite element analysis. Although their research object is analyzing the effects and structural response of different cushioning materials, rather than optimizing for the use of cushioning materials, their results confirm the influence of the thickness of the cushioning material on reducing the acceleration response. Therefore, we can effectively reduce the vibration response of the packaging system by changing the contact area and thickness of the unbalanced product. For unbalanced products, if there are special parts, they should be as far as possible placed at the center of mass end.

To better evaluate our results, we compare and discuss them with experimental results in the relevant literature. We refer to the work of Du et al. [21], which show that one can adjust the vibration response by changing the damping material. In their experiments, they find that the acceleration response can be effectively reduced by increasing the thickness and contact area of the damping material. This is consistent with our results. We also find that increasing the thickness of the damping material near the center of mass is more effective in reducing the amplitude of the acceleration response. However, our study points out that if the structure of the buffered packaging material cannot be changed due to product constraints, it can also be adjusted by changing the density of the buffered packaging damping material. This provides a new idea for the selection and design of damping materials. In addition, we also find that changing the damping coefficient of the damping material has an important effect on the dynamic characteristics of the packaging system. For the materials with larger damping coefficients, we observe that the acceleration response tends to decrease more significantly, especially near the eccentricity. This is consistent with the findings of Xue et al. [15] in 2022, who also find that the damping properties of the damping material have a significant effect on the vibration response.

Through above discussion, we validate our experimental results and provide clues to reveal these differences. These comparisons provide additional support for the reliability and practicality of our research and provide implications for future research directions.

6. Conclusions

This paper presented a method for correcting and adjusting the vibration response of mass-unbalanced products by changing the damping material. The main results can be summarized as follows:

(1) The acceleration response of the cushioning packaging system is influenced by the offset of the center of mass. In addition, the damping material will have a certain effect and can be used to correct the response.
(2) Without changing the damping material, the vibration response of the packaging system can be effectively reduced by changing both the contact area and thickness of the damping material for unbalanced products. Increasing the thickness of the damping material near the center of mass is more effective in reducing the acceleration-response amplitude. If the structure of the cushion packaging material cannot be changed due to product constraints, it can be adjusted through changing the density of the cushion packaging damping material.
(3) Changing the damping material and thus the damping coefficient of the package also influences the dynamic characteristics of the packaging system for non-equilibrium products, especially at the near eccentric end, where the acceleration response tends to decrease more significantly when using a material with a larger damping coefficient.
(4) When special parts are available for mass non-equilibrium products, they should be as far as possible placed at the mass center end.

This work provides a method for optimizing the structural parameters of cushioning packaging systems for products with unbalanced mass.

Author Contributions: Conceptualization, X.Y., Y.C., F.Z. and Y.S.; investigation, X.Y. and H.L.; writing—original draft preparation, H.L. and Y.C.; writing—review and editing, X.Y. and Y.S.; supervision, Y.C.; project administration, F.Z. and Y.C.; funding acquisition, Y.C., H.Z. and F.Z. All authors have read and agreed to the published version of the manuscript.

Funding: This work was supported by the Key Research and Development Program of Hubei Province of China (Grant No. 2020BBB084), National Natural Science Foundation of China (No. 52005168), the High Level Talent Fund of Hubei University of Technology (Grant No. BSQD2020010), the Open Fund of Hubei Key Laboratory of Modern Manufacturing Quality Engineering (Grant No. KFJJ2021012) and the Natural Science Foundation of Hubei Province (Grant No. 2022CFB882).

Institutional Review Board Statement: Not applicable.

Informed Consent Statement: Not applicable.

Data Availability Statement: The data used to support the findings of this study are available from the author upon request.

Acknowledgments: This work was supported by Xiaojun Yang, Yijie Cai and Fei Zhong.

Conflicts of Interest: The authors declare no conflict of interest.

References

1. Yang, J.; Long, R.; Chen, H.; Sun, Q. A comparative analysis of express packaging waste recycling models based on the differential game theory. *Conserv. Recycl.* **2021**, *168*, 105449. [CrossRef]
2. Fan, Z.; Wang, K. Current situation and application of plastic buffer packaging materials. *Plast. Packag.* **2022**, *32*, 7–11.
3. Lu, F.; Gao, D. Finite element analysis for anti-impact behavior of biogradable plant fibre bowls with foam cushioning packaging. *J. Vib. Shock.* **2015**, *34*, 137–139.
4. Lu, F.; Huang, G.; Wang, L.; Liu, Q.; Jiang, H.; Gao, D. Finite element analysis of dynamic compression response of trapezoidal polyethylene foam structure. *J. Vib. Shock.* **2019**, *38*, 234–238.
5. Zhong, C.; Yang, Y.; Zhou, L. Research status and prospect of E-commerce logistics packaging. *J. Packag.* **2020**, *12*, 27–34.
6. Csavajda, P.; Böröcz, P. Effect of Temperature Changes on the Vibration Transmissibility of XPE and PE Packaging Cushioning Material. *Appl. Sci.* **2021**, *11*, 482. [CrossRef]
7. Wang, X.; Chen, M.; Chen, J. Plastic shell type low voltage circuit breaker paper transport packaging design. *Packag. Eng.* **2020**, *41*, 88–94.
8. Zhu, D.; Gong, J. First pass damage analysis of displacement response of Single DOF packaging. *Packag. Eng.* **2017**, *38*, 68–73.
9. Li, H.; Chen, A. Drop Damage Evaluation of Wearing Parts of Suspension System. *Noise Vib. Control.* **2018**, *38*, 85–89.
10. Schell, E.H. Evaluation of a fragility test method and some proposals for simplified method. *Shock. Vib. Bull.* **1992**, *40*, 14–17.
11. Sun, Y.; Zhang, M. Nonlinear problems in packaging dynamics. *Packag. Eng.* **1995**, *16*, 6.
12. Li, H.; Wang, J.; Lu, L.; Wang, Z. An improved homotopy analysis method with accelerated convergence for nonlinear problems. *J. Vibroeng.* **2016**, *18*, 4756–4765. [CrossRef]
13. Duan, N.; Hao, M.; Chen, A. Damage Evaluation of Critical Components of Tilted Support Spring Nonlinear System under a Rectangular Pulse. *Math. Probl. Eng.* **2015**, *2015*, 910413. [CrossRef]
14. Sakara, G. The effect of axial force on the free vibration of an euler-bernoulli beam carrying a number of various concentrated elements. *Shock. Vib.* **2013**, *20*, 357–367.
15. Xue, Y.; Song, W.; Miao, H.; Wang, J.; Li, Y. Multi-Objective Optimal Design of Dropping Shock of Series Cushioning Packaging System. *Shock. Vib.* **2022**, *2022*, 9491102. [CrossRef]
16. Rong, H.; Yan, F.; Sun, D. Simulation Analysis on Vibration Mode of X-PLY Corrugated Paperboard in Transportation Engineering. *Adv. Mater. Res.* **2013**, *791*, 1084–1087.
17. Gao, D.; Lu, F. Study on shock response of cushion packaging system based on combined model using hyperbolic tangent and tangent functions with consideration of rotation effect. *Appl. Mech. Mater.* **2011**, *102*, 1161–1166. [CrossRef]
18. Kog, Y.C. Allowable eccentricity of pile groups for deep basements. *Pract. Period. Struct. Des. Constr.* **2023**, *28*, 04023002. [CrossRef]
19. Taha, A.E.; Elias, S.; Matsagar, V.; Jain, A.K. Seismic response control of asymmetric buildings using tuned mass dampers. *Struct. Des. Tall Spec. Build.* **2019**, *28*, 1541–7794. [CrossRef]
20. Du, Z.; Gao, W.; Kang, H. The Comparative Analysis of Cushion or Shock Absorption Characteristic of Commonly-Used Cushion Packaging Materials. *Adv. Mater. Res.* **2012**, *490*, 3902–3906. [CrossRef]
21. Cho, S.D.; Kim, J.M.; Kim, J.H.; Lee, K.W. Utilization of waste tires to reduce railroad vibration. *Mater. Sci. Forum.* **2007**, *544*, 637–640. [CrossRef]
22. Khalil, A.; Davoudpour, Y.; Saurabh, C.K.; Hossain, M.S.; Adnan, A.S.; Dungani, R.; Paridah, M.T.; Mohamed, Z.S.; Fazita, M.N.; Syakir, M.L.; et al. A review on nanocellulosic fibres as new material for sustainable packaging: Process and applications. *Renew. Sustain. Energy Rev.* **2016**, *64*, 823–836. [CrossRef]

23. Zhang, H. *Research on Optimization Design and Application of Buffer Packaging of Kitchen Electric Products*; Shanxi University of Science and Technology: Xi'an, China, 2019.
24. Li, Z.; Li, J.; Liu, F. Aluminum tray finite element analysis and optimization design. *J. Packag. Eng.* **2018**, *39*, 126–131.
25. Ge, C.F.; Priyadarshini, L.; Cormier, D.; Pan, L.; Tuber, J. A preliminary study of cushion properties of a 3D printed thermoplastic polyurethane Kelvin foam. *Packag. Technol. Sci.* **2018**, *31*, 361–368. [CrossRef]
26. Cai, W.; Li, B.; Wen, J.; Wang, L. Research on cushioning characteristics of airbag for UAV soft landing. *Acta Ordnance Eng.* **2014**, *35*, 1867–1875.
27. Qi, Y.; Li, W.; Zhu, W.; Yang, J.; Zeng, F.; Man, J. Research on landing buffer performance test method of lander. *Spacecr. Environ. Eng.* **2020**, *37*, 576–581.
28. Dong, C.; Zhang, Z.; Zhen, X.; Chen, M. Free Vibration of Summation Resonance of Suspended-cable-stayed Beam. *Math. Biosci. Eng.* **2019**, *16*, 7230–7249. [CrossRef]
29. Liang, N.; Guo, Y.; Wang, D. Finite element simulation analysis of vibration transmission characteristics of honeycomb paperboard. *Packag. Eng.* **2019**, *40*, 57–62.
30. Mi, N.; Li, G. Simulation analysis and optimization design of random vibration of analytical balance packaging. *J. Vib. Shock.* **2019**, *28*, 206–212.
31. Fadiji, T.; Ambaw, A.; Coetzee, C.J.; Berry, T.M.; Opara, U.L. Application of finite element analysis to predict the mechanical strength of ventilated corrugated paperboard packaging for handling fresh produce. *Biosyst. Eng.* **2018**, *174*, 260–281. [CrossRef]
32. Çeçen, F.; Aktaş, B. Modal and harmonic response analysis of new CFRP laminate reinforced concrete railway sleepers. *Eng. Failure Anal.* **2021**, *127*, 105471. [CrossRef]
33. *GB/T 8168−2008*; Testing Method of Static Compression for Packaging Cushioning Materials. Standards Press of China: Beijing, China, 2009.
34. Severn, R.T. The development of shaking tables—A historical note. *Earthq. Eng. Struct. Dyn.* **2011**, *40*, 195–213. [CrossRef]
35. Lepine, J.; Rouillard, V.; Sek, M. On the Use of Machine Learning to Detect Shocks in Road Vehicle Vibration Signals. *Packag. Technol. Sci.* **2017**, *30*, 387–398. [CrossRef]

Disclaimer/Publisher's Note: The statements, opinions and data contained in all publications are solely those of the individual author(s) and contributor(s) and not of MDPI and/or the editor(s). MDPI and/or the editor(s) disclaim responsibility for any injury to people or property resulting from any ideas, methods, instructions or products referred to in the content.